

Constraint on the growth factor of the cosmic structure from the damping of the baryon acoustic oscillation signature

Gen Nakamura^{1,*}, Gert Hütsi^{2,3,†}, Takahiro Sato^{1,‡} and Kazuhiro Yamamoto^{1,§}

¹*Department of Physical Science, Hiroshima University, Higashi-Hiroshima 739-8526, Japan*

²*Department of Physics and Astronomy, University College London, London, WC1E 6BT, UK*

³*Tartu Observatory, EE-61602 Tõrevere, Estonia*

We determine a constraint on the growth factor by measuring the damping of the baryon acoustic oscillations in the matter power spectrum using the Sloan Digital Sky Survey luminous red galaxy sample. The damping of the BAO is detected at the one sigma level. We obtain $\sigma_8 D_1(z=0.3) = 0.42_{-0.28}^{+0.34}$ at the 1σ statistical level, where σ_8 is the root mean square overdensity in a sphere of radius $8h^{-1}\text{Mpc}$ and $D_1(z)$ is the growth factor at redshift z . The above result assumes that other parameters are fixed and the cosmology is taken to be a spatially flat cold dark matter universe with the cosmological constant.

PACS numbers: 98.80.-k, 95.35.+d, 95.36.+x

I. INTRODUCTION

The baryon acoustic oscillations (BAO) are the sound oscillations of the primeval baryon-photon fluid prior to the recombination epoch. The BAO signature imprinted in the matter power spectrum is very useful for the study of the dark energy, hypothetically introduced to explain the accelerated expansion of the universe [1, 2], because the characteristic scale of the BAO plays a role of a standard ruler in the universe [3, 4, 5]. The BAO signature in the galaxy clustering is clearly detected [6, 7], and the constraints on the equation of state parameter of the dark energy are demonstrated [8, 9, 10, 11]. Future large surveys for the precise measurement of the BAO are in progress or planned, providing us an important tool to explore the origin of the accelerated expansion of the universe.

Besides the measurement of the BAO, those future surveys provide us other important information. For example, the redshift-space distortions will be measured precisely at the same time. The redshift-space distortions reflect the velocity of galaxies in the direction of the line of sight. Especially, the linear redshift-space distortion due to the Kaiser effect comes from the linear velocity field of matter perturbations, whose measurement will give us a chance to test the gravity theory on the cosmological scales [12, 13, 14, 15]. This is important because several modified gravity models are proposed to explain the accelerated expansion of the universe as an alternative to the dark energy. Thus the measurement of the redshift-space distortion, which is useful to constrain the growth rate and the growth factor of the cosmic structure, is also important.

In Ref. [16, 17], it is pointed out that the precise mea-

surement of the BAO may also be useful to constrain the growth factor. The BAO signature observed in the galaxy power spectrum is contaminated by the nonlinear effects of the density perturbations, redshift-space distortions and the clustering bias. The effects of the nonlinearity and the redshift-space distortions cause the damping of the BAO signature compared with the case when these effects are switched off. The authors of Ref. [16] found that the damping of the BAO depends on the amplitude of the matter power spectrum and that a measurement of the BAO damping might be useful to constrain the growth factor of the cosmic structure.

In Ref. [17], two of the authors of the present paper reported a detection of the BAO damping using the Sloan digital sky survey (SDSS) luminous red galaxy (LRG) sample of the data release (DR) 6. Since the observed galaxy power spectrum is contaminated by errors, and is noisy, the procedure of extracting the BAO signature from a galaxy power spectrum is a subtle problem. In the previous paper [17], the cubic spline method was used to construct a smooth power spectrum to extract the BAO signature. However, this method is very sensitive to parameters of the cubic spline, i.e., number and interval of the nodes. Due to those reasons, it is clear that an independent cross check of the previous result is useful.

In the present paper, we adopt an independent method to construct the smooth power spectrum, which is stable compared with the cubic spline method, and re-investigate the BAO damping by confronting the model predictions with the SDSS LRG power spectrum of the DR7. We confirm the detection of the BAO damping at the one sigma level. Also we obtain a constraint on the parameter combination $D_1(z)\sigma_8$ at the redshift $z = 0.3$ from the BAO damping for the first time. Here $D_1(z)$ is the growth factor and σ_8 is the amplitude of the root mean square overdensity in a sphere of radius $8h^{-1}\text{Mpc}$. We denote the growth rate by $f(z) = d \ln D_1(z) / d \ln a(z)$, where $a(z)$ is the scale factor. Throughout this paper, we use units in which the velocity of light equals 1 and the Hubble parameter $H_0 = 100h\text{km/s/Mpc}$ with $h = 0.7$.

*Email: gen@theo.phys.sci.hiroshima-u.ac.jp

†Email: ghutsi@star.ucl.ac.uk

‡Email: sato@theo.phys.sci.hiroshima-u.ac.jp

§Email: kazuhiro@hiroshima-u.ac.jp

II. BAO DAMPING

The BAO signature in the power spectrum $P(k)$ can be obtained by

$$B(k) \equiv \frac{P(k)}{\tilde{P}(k)} - 1, \quad (1)$$

where $\tilde{P}(k)$ represents the 'smooth' power spectrum corresponding to $P(k)$. Since the definition of $\tilde{P}(k)$ is not unique, the construction of $\tilde{P}(k)$ should be carefully done. The cubic spline method is frequently used [9, 17], but it is not always stable if dealing with a noisy power spectrum from observations.

In the present paper, we construct the smooth power spectrum as the linear matter power spectrum multiplied by a simple analytic function of the wave number. With the use of the constructed smooth power spectrum, we obtain the BAO signature from the SDSS LRG power spectrum of the DR7 [19, 20]. The extracted BAO signature is then compared with theoretical predictions, particularly focusing on the BAO damping.

We use the SDSS LRG sample from DR 7 (see also [21, 22] for recent results on LRGs from the SDSS DR7). Our LRG sample is restricted to the redshift range $z = 0.16 - 0.47$. In order to reduce the sidelobes of the survey window we remove some noncontiguous parts of the sample (e.g. three southern slices), which leads us to ~ 7150 deg² sky coverage with a total of 100157 LRGs. The data reduction procedure is the same as that described in Ref. [6]. In this power spectrum analysis, we adopted the spatially flat Lambda cold dark matter (Λ CDM) model distance-redshift relation $s = s[z]$. Figure 1 shows the observed power spectrum $P_{\text{obs}}(k)$.

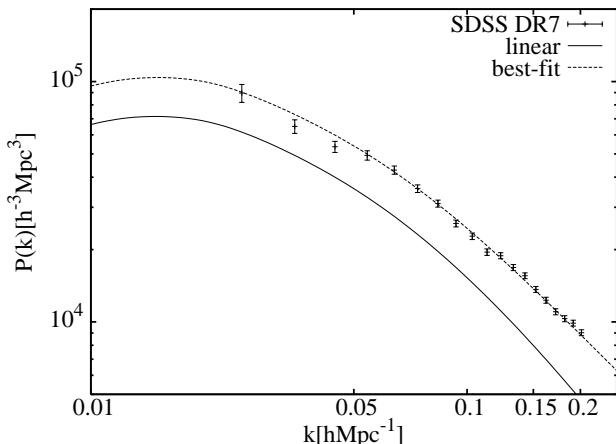


FIG. 1: Comparison of the SDSS LRG power spectrum and the theoretical power spectra. The solid curve is the linear theory $\tilde{P}_{\text{lin}}(k)$. The dashed curve is a 'smooth' power spectrum $\tilde{P}_{\text{obs}}(k)$ obtained with (3) with the Case 3. The cosmological parameters are described in Table I labeled as model no.1.

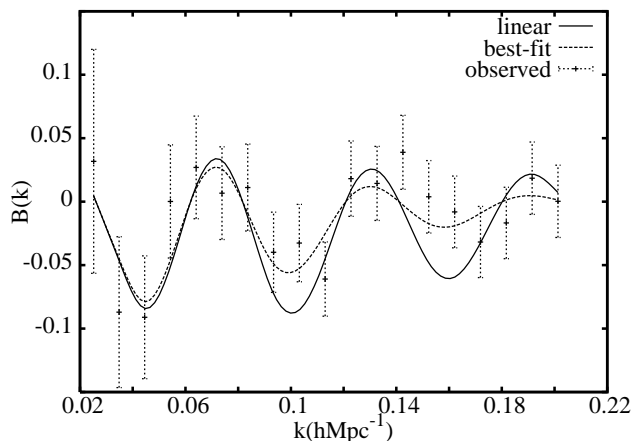


FIG. 2: The BAO signature $B(k)$. The solid curve is the BAO in linear theory $B_{\text{lin}}(k)$. The dashed curve is the best fit theoretical curve including the damping $B_{\text{lin}}(k)(1 - W(k))$. The points with error bars are $B_{\text{obs}}(k_i)$, the observational result obtained with the Case 3 for $A(k)$. We adopted the cosmological density parameters and the spectral index described in Table I as model no.1.

The observed power spectrum is contaminated by various effects: the nonlinear effect, redshift-space distortions, clustering bias, and so on. In particular, the modeling of the clustering bias seems to be very difficult, because it depends on the galaxy formation process. In the present paper, in order to construct the smooth power spectrum corresponding to the observed power spectrum, we assume

$$\tilde{P}_{\text{obs}}(k) = A^2(k)\tilde{P}_{\text{lin}}(k), \quad (2)$$

where $\tilde{P}_{\text{lin}}(k)$ is the linear no-wiggle power spectrum of [1]. The solid curve and the dashed curve in Fig. 1 exemplify $\tilde{P}_{\text{lin}}(k)$ and $\tilde{P}_{\text{obs}}(k)$, respectively.

We determined the function $A(k)$ as follows: We first define the chi-square by

$$\begin{aligned} \chi^2 = & \sum_{i,j} [B_{\text{lin}}(k_i)(1 - W(k_i)) - B_{\text{obs}}(k_i)] \\ & \times \tilde{P}_{\text{obs}}(k_i) \text{Cov}^{-1}(k_i, k_j) \tilde{P}_{\text{obs}}(k_j) \\ & \times [B_{\text{lin}}(k_j)(1 - W(k_j)) - B_{\text{obs}}(k_j)] \end{aligned} \quad (3)$$

with

$$B_{\text{lin}}(k) = \frac{P_{\text{lin}}(k)}{\tilde{P}_{\text{lin}}(k)} - 1, \quad (4)$$

$$B_{\text{obs}}(k) = \frac{P_{\text{obs}}(k)}{\tilde{P}_{\text{obs}}(k)} - 1, \quad (5)$$

where $\text{Cov}^{-1}(k_i, k_j)$ is the inverse of the power spectrum covariance matrix [8], and $W(k)$ is the damping function (see next section for details). In the determination of $A(k)$, we consider the following 3 cases,

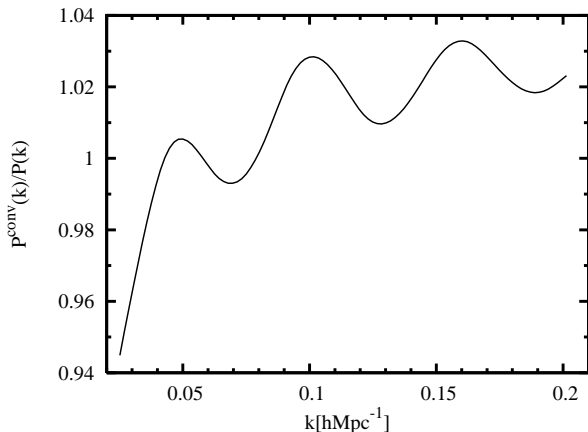


FIG. 3: Ratio of the power spectrum convolved with the window function $P^{\text{conv}}(k)$ to that without it $P(k)$. The cosmological parameters are the same as those of Fig.1.

Case 1 We assume $A(k) = a + bk + ck^2$ and determine a, b and c by minimising (3) with $f = 0$, $\sigma_8 D_1 = 0$ (corresponding to no-damping model).

Case 2 Same as Case 1 but with $f = 0.64$, $\sigma_8 D_1 = 0.53$ (corresponding to the Λ CDM model with $\Omega_0 = 0.28$).

Case 3 We assume $A(k) = a + bk^c$ and determine a, b and c by minimizing (3) separately for each of the adopted cosmologies.

Fig.2 shows an example of the observed BAO signature and theoretical curves, which will be explained in the next section. Here the cosmological parameters are the same as those of Fig. 1.

Here we note the effect of the window function, which we take into account in our investigation. This is the finite volume effect of the region where galaxies are distributed, depending on the data analysis as well. The effect of the window function affects the shape of the BAO signature, which is not negligible in our investigation. The details are described in the literature [6, 23]. Fig.3 shows the ratio of the power spectrum convolved with the window function to that without it.

III. THEORETICAL MODELING OF THE BAO DAMPING

In our theoretical modeling, we adopt the quasi-nonlinear power spectrum using the technique of resumming infinite series of higher order perturbations on the basis of the Lagrangian perturbation theory (LPT), which was proposed by Matsubara [18]. One of the advantages of using this LPT formalism is that the redshift-space distortions can be taken into account. Furthermore, the predicted BAO signature was compared with the results

of N-body simulations in [17], where a good agreement was obtained.

We denote the matter power spectrum in the redshift-space by $P(k, \mu)$, where μ is the cosine of the angle between the line of sight direction and the wave number vector. However, the observed power spectrum in the previous section is the angular averaged power spectrum, which is related to $P(k, \mu)$ via

$$P(k) = \frac{1}{2} \int_{-1}^{+1} P(k, \mu) d\mu. \quad (6)$$

Then, the BAO signature is written as

$$B(k) \equiv \frac{\int_{-1}^{+1} P(k, \mu) d\mu}{\int_{-1}^{+1} \tilde{P}(k, \mu) d\mu} - 1. \quad (7)$$

The BAO damping is described by the function $W(k)$, which is defined by

$$B(k) = (1 - W(k)) B_{\text{lin}}(k) \quad (8)$$

where $B_{\text{lin}}(k)$ is the BAO in the linear theory defined by Eq. (4). Note that $B_{\text{lin}}(k)$ does not depend on the redshift z because the growth factor in the linear power spectrum cancels. We may define the angular dependent damping factor $W(k, \mu)$ by

$$\frac{P(k, \mu)}{\tilde{P}(k, \mu)} - 1 = (1 - W(k, \mu)) B_{\text{lin}}(k), \quad (9)$$

which leads to

$$W(k) = \frac{\int_{-1}^1 d\mu W(k, \mu) \tilde{P}(k, \mu)}{\int_{-1}^1 d\mu \tilde{P}(k, \mu)}. \quad (10)$$

Following the LPT framework [5], the matter power spectrum in the redshift-space is a function of μ and the redshift z , which we denote by $P_{\text{LPT}}(k, \mu, z)$. To calculate $P_{\text{LPT}}(k, \mu, z)$ one needs the linear matter power spectrum in redshift space, which depends on $\sigma_8 D_1(z)$, the growth factor multiplied by the normalization factor, and the growth rate $f(z) = d \ln D_1(z) / d \ln a(z)$, where $a(z)$ is the scale factor. The full expression for $P_{\text{LPT}}(k, \mu, z)$, which is rather complicated, can be found in Ref. [5].

In the previous work [17], it was found that the angular dependent damping function at the redshift z is approximately given by

$$\mathcal{W}(k, \mu; z) = \frac{D_1^2(z)}{1 + \alpha(\mu, z) D_1^2(z) \tilde{g}(k)} \frac{\tilde{P}_{22}^{(s)}(k, \mu)}{\tilde{P}_{\text{lin}}^{(s)}(k, \mu)}, \quad (11)$$

where $P_{\text{lin}}^{(s)}(k, \mu) = (1 + f\mu^2)^2 P_{\text{lin}}(k)$, $\alpha(\mu, z) = 1 + f(f + 2)\mu^2$, $\tilde{g}(k) = (k^2/6\pi^2) \times \int_0^\infty dq P_{\text{lin}}(q)$, and $P_{(s)22}^{(s)}(k, \mu)$ is the function to describe the higher order corrections in the LPT framework, which is given in Appendix B of Ref. [5], but note that the 'tilde' means the quantity with the no-wiggle linear power spectrum.

In the present paper, we adopt $\mathcal{W}(k, \mu = 0.65, z = 0.3)$ as the theoretical damping function $W(k)$ to be compared with observations. Here $z = 0.3$ is a mean redshift of the LRG sample. Also, the angular averaged damping function defined by Eq. (10) is well approximated by $\mathcal{W}(k, \mu = 0.65, z = 0.3)$, which is demonstrated in Figure 4. The solid curve is the angular averaged damping function Eq. (10), the dotted curve is $\mathcal{W}(k, \mu = 0.65, z = 0.3)$.

In summary, the damping function $W(k)$ depends on the linear matter power spectrum and the growth rate $f(z)$ at the mean redshift $z = 0.3$. Then, by comparing the BAO damping with observations, we can hope to constrain $\sigma_8 D_1(z)$ and $f(z)$.

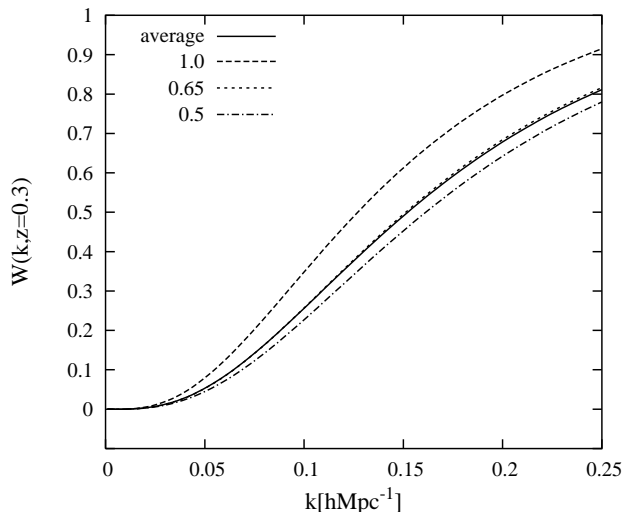


FIG. 4: The damping function $\mathcal{W}(k, \mu; z)$ at redshift $z=0.3$ as a function of the wave number, for $\mu = 0.5$ (dot dashed), 0.65 (dotted) and 1.0 (long dashed), respectively. The solid curve is the angular averaged damping function Eq. (10). The cosmological parameters are described in Table I labeled as model no. 1.

IV. COMPARISON BETWEEN OBSERVATION AND THEORY

We compare the observational result and the theory by calculating the chi-square defined by Eq. (3) with the function $A(k)$ determined by the methods in section 2. In our analysis, we treat f and $\sigma_8 D_1$ as independent variables which have nothing to do with the cosmological parameters. Figure 5 is the contour of $\Delta\chi^2$ at 1σ level on the $\sigma_8 D_1$ - f plane, where the other parameters are fixed as $\Omega_0 = 0.28$, $\Omega_b = 0.046$ and the spectral index $n_s = 0.96$. The best fit value is $\sigma_8 D_1 = 0.40$ and $f = 0.76$, but the BAO damping is not very sensitive to the growth rate f .

Figure 6 shows the likelihood as a function of $\sigma_8 D_1$, where the parameter f is integrated over the range $0 \leq f \leq 2$.

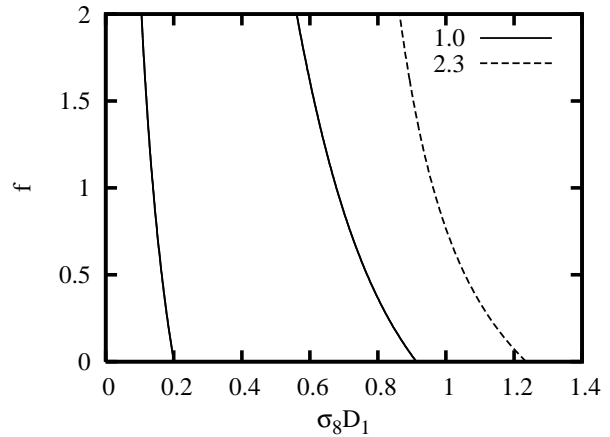


FIG. 5: The contour of $\Delta\chi^2 = 1.0, 2.3$ on the $\sigma_8 D_1$ - f plane with Case 3. The other cosmological parameters are fixed as those of model no. 1. in Table I.

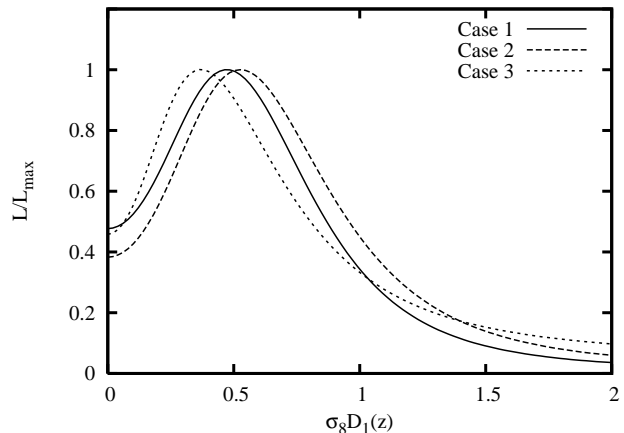


FIG. 6: The likelihood as a function of $\sigma_8 D_1$ with f integrated over the range $0 \leq f \leq 2$. The cosmological parameters are fixed as those of model no. 4. in Table I.

Table I shows the results of the chi-squared test Eq. (3) for various cosmological parameters. For the consistency of the analysis, we used the data of $P_{\text{obs}}(k)$, which was calculated adopting the distance redshift relation $s = s[z]$ of the same cosmological parameters. From this table, it is clear that finite positive values of $\sigma_8 D_1 > 0$ better fit the data for all the models. This allows us to conclude that the detection of the BAO damping is at the 1σ level at the worst case. The Λ CDM model with $\Omega_0 = 0.28$ predicts $D_1(z = 0.3) \sim 0.65$. If we adopt the value of $\sigma_8 = 0.8$ from Ref. [24], we have $\sigma_8 D_1 \sim 0.53$. This is consistent with our result within the 1σ level.

To discuss the attainable constraints on $\sigma_8 D_1(z)$ in future observations, we calculate the relevant Fisher matrix

component

$$F = \frac{1}{4\pi^2} \int_{k_{\min}}^{k_{\max}} dk k^2 \left(\frac{\partial B(k, z)}{\partial (\sigma_8 D_1)} \right)^2 \frac{\tilde{P}_{\text{gal}}^2(k, z)}{Q^2(k, z)}, \quad (12)$$

where we set $k_{\max} = 0.2$, $k_{\min} = 0.02$, $B(k, z) = (1 - \mathcal{W}(k, \mu = 0.65), z) B_{\text{lin}}(k)$, $\tilde{P}_{\text{gal}}(k, z)$ is the galaxy power spectrum and $Q(k, z) = \Delta A \int_{z_{\min}}^{z_{\max}} dz (ds/dz) s^2 \bar{n}^2 / [1 + \bar{n} P_{\text{gal}}(k, z)]^2$ with the mean number density of galaxies \bar{n} and the survey area ΔA . We adopted the Q-model for the galaxy power spectrum, elaborated in [25] with the parameters $A_1 = 1.4$ and $Q = 16$ (see also [16]).

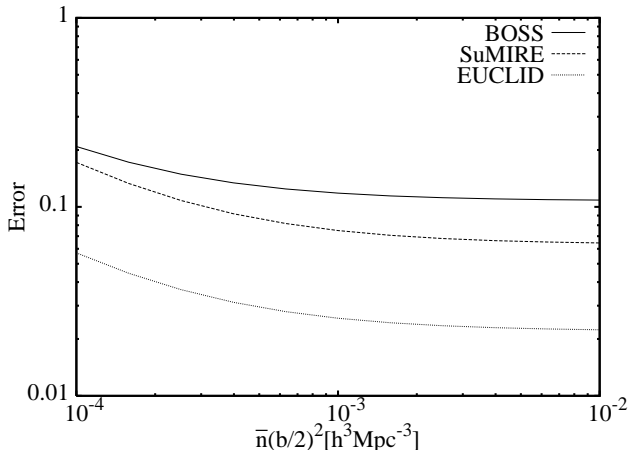


FIG. 7: The 1σ -level statistical errors of $\sigma_8 D_1(z)$ as a function of $\bar{n}(b/2)^2$ with the constant number density \bar{n} and the bias b .

The minimum error attainable on $\sigma_8 D_1$ is given by $1/F^{1/2}$. Figure 7 shows $1/F^{1/2}$ as a function of $\bar{n}(b/2)^2$,

where b is the bias parameter of the Q-model. For the future surveys, we adopted the parameters in Table II [15, 26, 27]. We computed the constraint at the mean redshift $z = (z_{\max} + z_{\min})/2$ for each survey. The minimum error $\sigma_8 D_1$ is typically 0.1, but depends on the mean number density and the clustering bias.

V. SUMMARY AND CONCLUSIONS

In this work, we examined the BAO damping. We used the observed power spectrum of the SDSS LRG sample of DR7. The result shows that the BAO damping really exists and a constraint on $\sigma_8 D_1$ is obtained for the first time from the damping. The detection of the BAO damping is robust, and do not depend much on the specific model used to define the smooth model. The constraint on $\sigma_8 D_1$ is note very tight, but this is an independent and unique test for the growth factor. Furthermore, this method might be useful for future surveys [17].

In the present analysis, we have not considered the effect of the clustering bias on the BAO damping. This point might be considered more carefully in the future.

Acknowledgements

We thank H. Nomura and T. Nishimichi for useful suggestions and comments. This work was supported by a Grant-in-Aid for Scientific research of Japanese Ministry of Education, Culture, Sports, Science and Technology (No. 21540270). This work is supported in part by Japan Society for Promotion of Science (JSPS) Core-to-Core Program, International Research Network for Dark Energy. We used the CAMB code for computation of the wiggle power spectrum [28].

-
- [1] D.J. Eisenstein and W. Hu, *Astrophys. J.* **496**, 605 (1998)
 - [2] A.Meiksin, M.White, and J.A. Peacock, *Mon. Not. R. Astron. Soc.* **304**, 851 (1999)
 - [3] D.J. Eisenstein, W. Hu, and M. Tegmark, *Astrophys. J. Lett.* **504**, L57 (1998)
 - [4] H.J. Seo, D.J. Eisenstein, *Astrophys. J.* **598**, 720 (2003)
 - [5] T. Matsubara, *Astrophys. J.* **615**, 573 (2004)
 - [6] G. Hütsi, *Astron. Astrophys.* **449**, 891 (2006)
 - [7] W.J. Percival, *et al.*, *Astrophys. J.* **657**, 51 (2007); *Astrophys. J.* **657**, 645 (2007)
 - [8] G. Hütsi, *Astron. Astrophys.* **459**, 375 (2006).
 - [9] W.J. Percival *et al.*, *Mon. Not. R. Astron. Soc.* **381**, 1053 (2007)
 - [10] T. Okumura *et al.*, *Astrophys. J.* **676**, 889 (2008)
 - [11] A. Cabre ad E. Gaztanaga, *MNRAS* **393** 1183 (2009)
 - [12] E. V. Linder, *Astropart. Phys* **29**, 336 (2008)
 - [13] L. Guzzo *et al.*, *Nature (London)*. **451**, 541 (2008)
 - [14] K. Yamamoto, T. Sato, and G. Hütsi, *Prog. Theor. Phys.* **120**, 609 (2008).
 - [15] M. White, Y-S Song, W. J. Percival, arXiv:0810.1518
 - [16] H. Nomura, K. Yamamoto, and T. Nishimichi, *J. Cosmol. Astropart. Phys.* **10** (2008) 031.
 - [17] H. Nomura *et al.*, *Phys Rev. D* **79**, 063512 (2009)
 - [18] T. Matsubara, *Phys Rev. D* **77**, 063530 (2008)
 - [19] D.J. York *et al.*, *AJ*, **120**, 1579 (2000)
 - [20] K. Abazajian *et al.*, *Astrophys. J. Supp.* **182**, 543 (2009)
 - [21] W. J. Percival *et al.*, arXiv:0907.1660
 - [22] B. A. Reid *et al.*, arXiv:0907.1659
 - [23] T. Sato, *et al.*, in preparation
 - [24] E. Komatsu *et al.*, *Astrophys. J. Suppl.* **180**, 330 (2009)
 - [25] A. G. Sanchez, C. M. Baugh, R. Angulo *MNRAS* **390**, 1470 (2008)
 - [26] <http://www.sdss3.org/index.php>
 - [27] H. Aihara, talk at the IPMU international conference on dark energy: lighting up the darkness!
 - [28] A. Lewis, A. Challinor, A. Lasenby, *Astrophys. J.* **538**, 473 (2000); <http://camb.info/>

No.	Ω_m	Ω_b	n_s	f	$\sigma_8 D_1(1\sigma \text{ level})$ Case 1	Case 2	Case 3
1	0.28	0.046	0.96	0.64	$0.38^{+0.26}_{-0.26}$	$0.42^{+0.30}_{-0.24}$	$0.42^{+0.34}_{-0.28}$
2	0.28	0.046	0.96	0.60	$0.38^{+0.27}_{-0.25}$	$0.42^{+0.30}_{-0.24}$	$0.42^{+0.33}_{-0.27}$
3	0.28	0.046	0.96	0.70	$0.37^{+0.26}_{-0.24}$	$0.40^{+0.30}_{-0.22}$	$0.41^{+0.32}_{-0.26}$
4	0.28	0.046	0.96	integrated	$0.48^{+0.30}_{-0.30}$	$0.52^{+0.36}_{-0.30}$	$0.38^{+0.38}_{-0.28}$
5	0.27	0.046	0.96	0.64	$0.44^{+0.25}_{-0.21}$	$0.46^{+0.28}_{-0.20}$	$0.56^{+0.40}_{-0.24}$
6	0.29	0.046	0.96	0.64	$0.36^{+0.32}_{-0.32}$	$0.42^{+0.35}_{-0.28}$	$0.50^{+0.36}_{-0.26}$
7	0.28	0.048	0.96	0.64	$0.38^{+0.26}_{-0.21}$	$0.42^{+0.28}_{-0.21}$	$0.42^{+0.32}_{-0.22}$
8	0.28	0.044	0.96	0.64	$0.36^{+0.29}_{-0.28}$	$0.42^{+0.31}_{-0.27}$	$0.40^{+0.36}_{-0.30}$
9	0.28	0.046	0.98	0.64	$0.40^{+0.30}_{-0.24}$	$0.46^{+0.32}_{-0.26}$	$0.42^{+0.33}_{-0.26}$
10	0.28	0.046	0.94	0.64	$0.34^{+0.25}_{-0.24}$	$0.38^{+0.27}_{-0.22}$	$0.40^{+0.32}_{-0.26}$

TABLE I: The results of the chi-squared test of the BAO damping for various cosmological models. In the table, 'integrated' means that f is integrated over the range $0 \leq f \leq 2$.

Survey	z_{\min}	z_{\max}	$\bar{n}[h^3 \text{Mpc}^{-3}]$ (Typical value)	Area $\Delta A[\text{deg.}^2]$
BOSS	0.1	0.7	3×10^{-4}	10^4
SuMIRE	0.7	1.6	4×10^{-4}	2×10^3
EUCLID	0.1	2	5×10^{-3}	2×10^4

TABLE II: Future survey parameters adopted in the Fisher matrix analysis.